

Soft Soil Overconsolidation and CPTU Dissipation Test

Lech Bałachowski

Gdańsk University of Technology, Faculty of Civil and Environmental Engineering,
ul. G. Narutowicza 11/12, 80-952 Gdańsk, Poland, e-mail: abal@pg.gda.pl

(Received October 07, 2005; revised March 17, 2006)

Abstract

Stress state and stress history of subsoil under the flood embankment was evaluated with CPTU and DMT tests. The CPTU dissipation tests in soft soils under the central part of the embankment and on the upstream and downstream sides were performed. The shape of pore water dissipation curve reflects stress state and stress history. Monotonic decay of water pore pressure was found for normally consolidated soils. Dilatory pore pressure response is typical for overconsolidated soils. Methods for the flow characteristics determination (coefficient of consolidation and hydraulic conductivity) were presented.

Key words: CPTU, DMT, pore pressure, stress history, soft soil

1. Introduction

Characterization of soft soils with modern in-situ tests is becoming a common practice. Cone penetration test with pore pressure measurements (CPTU) together with dilatometer test (DMT) permit a reliable and comprehensive evaluation of soft soil parameters (Mayne 2001, Młynarek 2003, 2004). With large strains produced during CPTU probe insertion, the soil resistance is determined. Moderate strain level around DMT blade enables the stress state and soil deformability to be evaluated. Moreover, the complementary character of both tests is supplemented with a dissipation test. As the CPTU penetration in less permeable soils is held in undrained conditions, the pore pressure is generated around the probe. When the penetration is stopped at a given depth, one can monitor the dissipation of the induced pore pressure to the hydrostatic one. Two shapes of the dissipation curve, i.e. monotonic decay or dilatory pore pressure response are recorded, related to the soil stress state and history. During this test the flow characteristics of cohesive or organic soil can be estimated. Enhanced in-situ tests with DMT and CPTU completed with dissipation tests were performed for the flood embankments of the Vistula river in the Żuławy Lowland.

2. Subsoil Characterization with CPTU and DMT Soundings

A series of CPTU and DMT soundings was performed at the crown and at the upstream and downstream toe of the flood embankments in order to characterize its corps and the parameters of soft soils in the subsoil. The embankment itself is generally built from silty soils, like sandy silts, silty or sandy clay, clayey silts or sands, silty sand and silts, and it can also contain some clay layers or fine sand. The height of the embankment in the analysed section is about 7.0 m. In the subsoil, one can distinguish a superficial clayey layer with some organic content, covering sandy or silty mud and a local peat layer. Some sandy interbeddings can be found in the mud. At the bottom fine and medium sands were deposited. An example of the flood embankment is given in Fig. 1. The CPTU and DMT tests were made with Geotech 220 rig, property of Gdańsk University of Technology. The soundings were performed from the crown of the embankment and at the toe from the upstream and downstream sides.

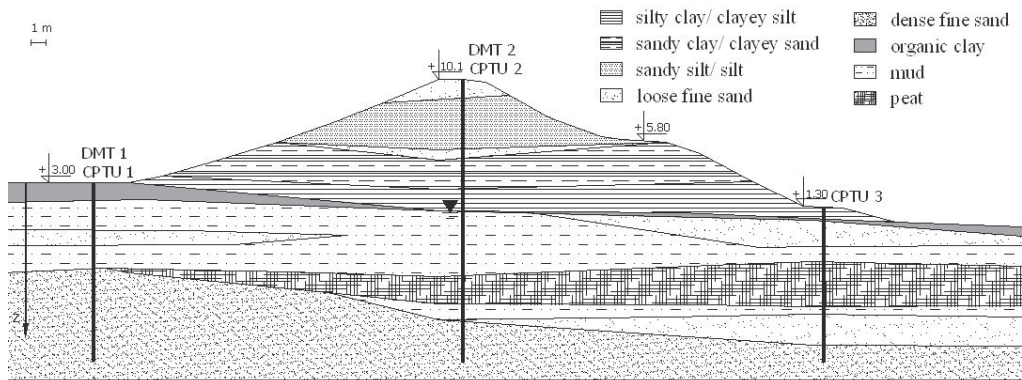


Fig. 1. Flood embankment and geotechnical cross-section

Attention was focused on the stress state in the subsoil and on the flow characteristics of the soft organic layers. The compaction of the embankment itself, its permeability, shear strength of the subsoil and safety analysis are beyond the scope of this paper.

Classical CPTU probe with pore pressure u_2 measurement was used. The readings of cone resistance q_c , sleeve friction f_s and pore pressure measurements u_2 performed in the embankment subsoil from the crown and at the toe from the upstream and downstream sides are given in Fig. 2. For comparison the measurements in the core of the embankment were omitted on this figure and the results are presented from the reference level, i.e. the elevation of the embankment toe on the upstream side. For the test on the downstream side the measurements were recorded from 1.7 m below this reference level.

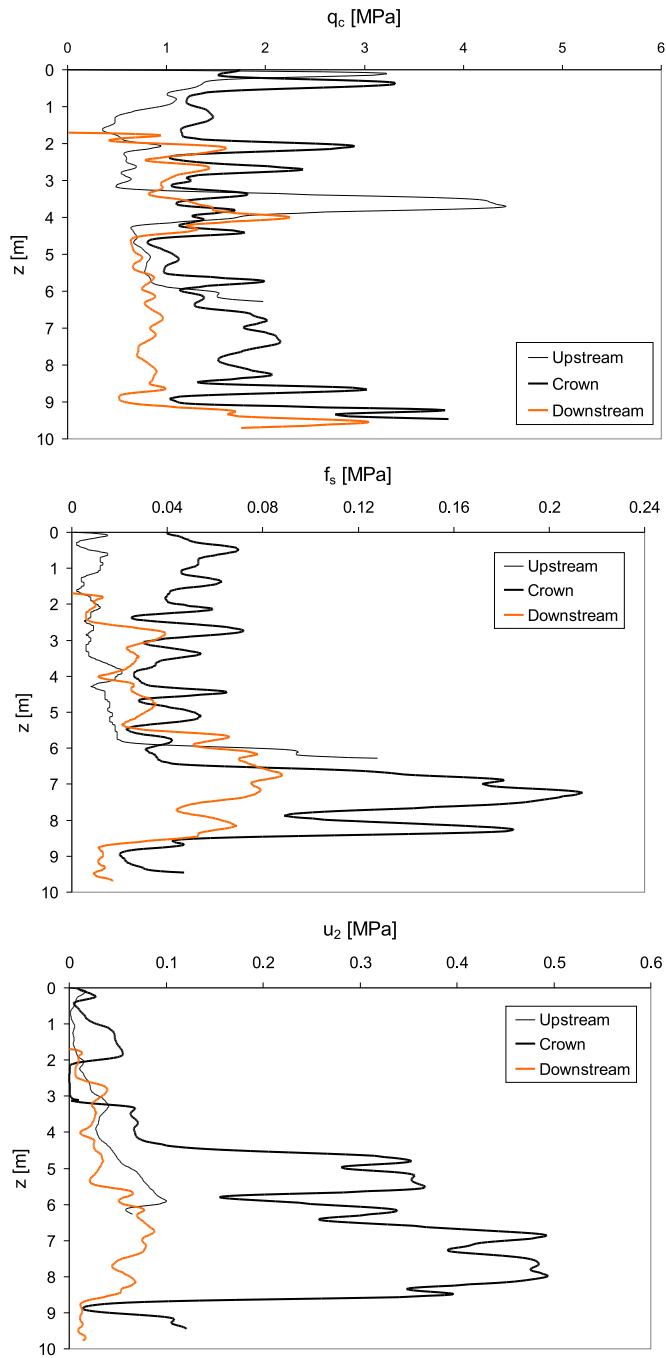


Fig. 2. CPTU profiles for the soundings from the crown, upstream and downstream toe of the embankment



Due to crust phenomena one can already observe a relatively small cone resistance (from 0.5 to 1.8 MPa) mobilized in clayey layers from the very beginning of penetration. Pore pressure measurements are influenced by the local thin inclusions of dense sands or by recent and ancient crust layers, being structurally overconsolidated. The recorded pore pressure drops after the passage of a such layer. In less permeable zones, pore pressures higher than the hydrostatic one are mobilized, especially under the central part of the embankment. According to Marchetti et al (2004) the pore pressure measured by CPTU is recorded in the soil annulus of the small volume surrounding the filter. Occasionally, it could reflect unrepresentative soil behaviour, especially in highly heterogeneous, stratified or even laminated alluvial soils with very contrasted soil characteristics. The CPTU data presented in Fig. 2 are filtrated. The cone resistance q_c , friction ratio F_r together with the results of borings were used to delineate the soil strata within the subsoil. While the data filtration can be useful for the determination of the average soil parameters it could, however, mask some important details of the soil structure. The laminations within alluvial soil will considerably change the soft soil response during dissipation tests. Careful analysis of non-filtrated data are thus essential in the proper analysis and the interpretation of CPTU dissipation curve. A series of CPTU dissipation tests was performed in the mud under the central part of the embankment and at the upstream and downstream sides. The analysis of dissipation of the excess water pressure mobilized during CPTU probe insertion needs a good knowledge of general drainage conditions. However, in very heterogeneous alluvial soils under the embankment, the presence of local seams or inclusions of more permeable material will be even more relevant to the analysis of dissipation tests.

Some dilatometer tests were realized in the vicinity of CPTU soundings. The DMT blade was pushed into the soil with Geotech 220 rig and the measurements were taken each 20 cm. A and B gas pressures were registered, corrected p_0 and p_1 pressures were calculated and three intermediate parameters were obtained (Marchetti 1980):

- material index

$$I_D = \frac{p_1 - p_0}{p_0 - u_0}, \quad (1)$$

- lateral stress index

$$K_D = \frac{p_0 - u_0}{\sigma'_{v0}}, \quad (2)$$

- dilatometer modulus



$$E_D = 34.7(p_1 - p_0), \quad (3)$$

where:

- u_0 – hydrostatic pressure,
- σ'_{v0} – effective overburden stress.

The material index I_D is used to estimate soil type, the lateral stress index K_D reflects stress history of the soil and can be regarded as earth pressure coefficient K_0 amplified by the penetration (Marchetti et al 2001). Profile of K_D resembles OCR profile, with K_D value equal to 2 corresponding to normally consolidated cohesive soils. One should remember that material index I_D is not related to soil granulometry but reflects the soil behavior and can be considered as some kind of rigidity index (Marchetti et al 2001). The dilatometer modulus E_D is obtained from p_0 and p_1 by the theory of elasticity.

One of the major advantages of DMT test is the possibility to evaluate vertical drained constrained modulus (Marchetti 1980):

$$M_{DMT} = R_M E_D, \quad (4)$$

where:

- R_M – empirical coefficient dependent on I_D and K_D .

Two diagrams with interpreted DMT soundings, performed in the same section of the embankment as CPTU tests, at the crown and at the upstream toe are given in Fig. 3. The data from the embankment body are omitted on this diagram and the profiles begin from the same reference level – at the upstream embankment toe – as for CPTU tests. The first profile to be analyzed by an engineer is K_D (Marchetti et al 2001). K_D values close to 2 are observed in the subsoil under the embankment as the weight of the embankment exceeded the existing preconsolidation pressure in the soft soil under the central part of the embankment. Higher K_D values are found in the subsoil at the embankment toe. Soft soil under the central part of the embankment is thus normally consolidated, while the soil at the embankment toe is overconsolidated. This overconsolidation can be related to ground water fluctuations, complex stress history during embankment construction and to lateral stress increase in the subsoil, due to embankment load. Apart from mechanical overconsolidation a structural overconsolidation can be observed in organic soils (Wolski 1988).

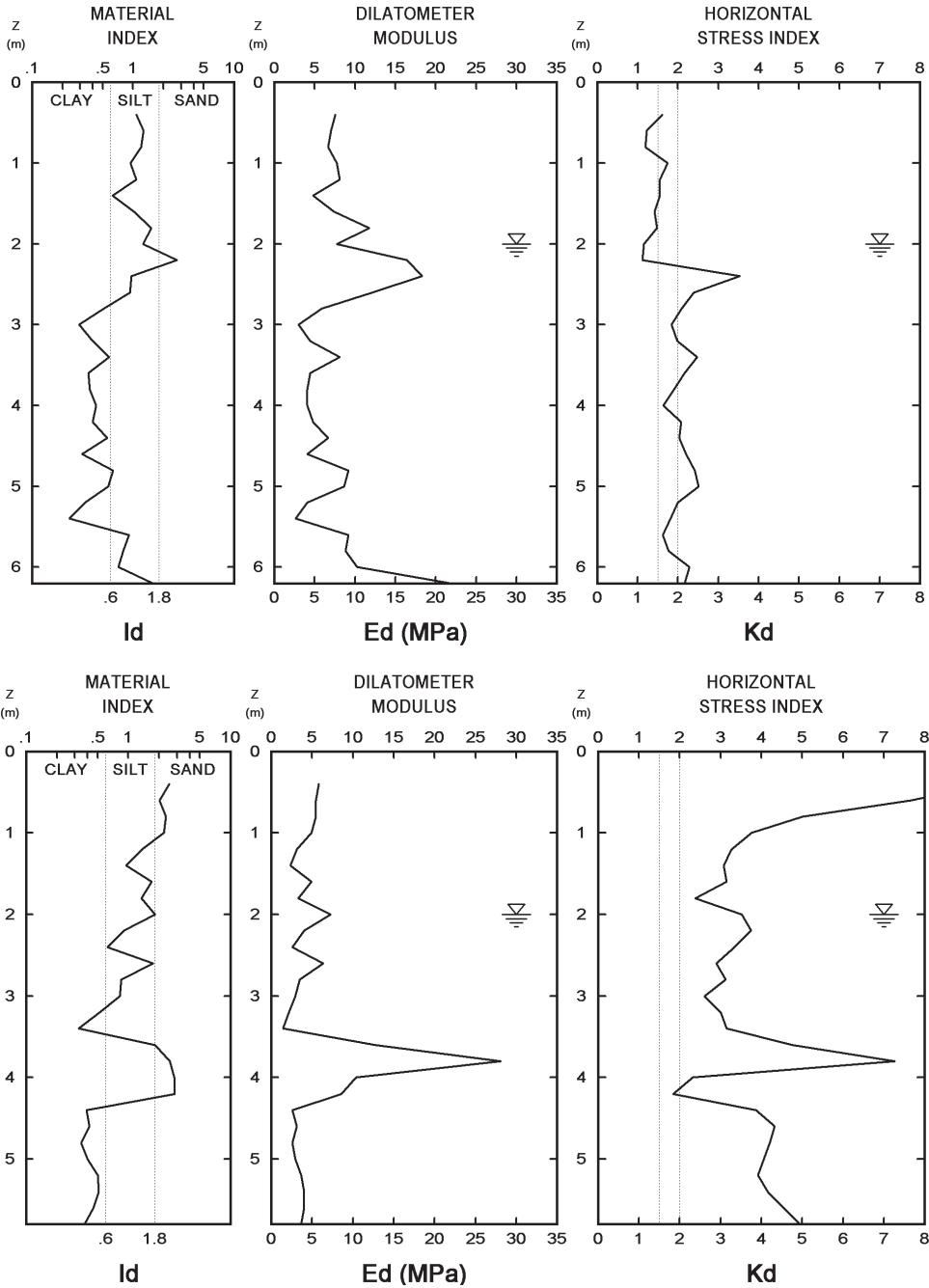


Fig. 3. DMT results for the soundings under the central part (upper diagram) and in the upstream toe of the embankment (lower diagram)



3. Evaluation of Stress State and History in the Subsoil

3.1. Soft Soil Consolidation

The soft subsoil under the flood embankment was already subjected to long term consolidation in good drainage conditions and is characterized by the inclusions of sandy layers and seams, so the consolidation process seems to be completed. In order to verify this hypothesis, the criterion established by Tanaka and Sakagami (1989) was checked (Fig. 4) using the pore pressure measurements in CPTU tests. In normally consolidated clays the pore pressure difference Δu is equal (Tanaka and Sakagami 1989):

$$\Delta u = u_{\max} - u_0 = 0.75(q_t - \sigma_{v0}), \quad (5)$$

where:

- u_{\max} – the maximum registered pore pressure,
- u_0 – hydrostatic pore pressure at given depth,
- q_t – corrected cone resistance,
- σ_{v0} – total overburden stress.

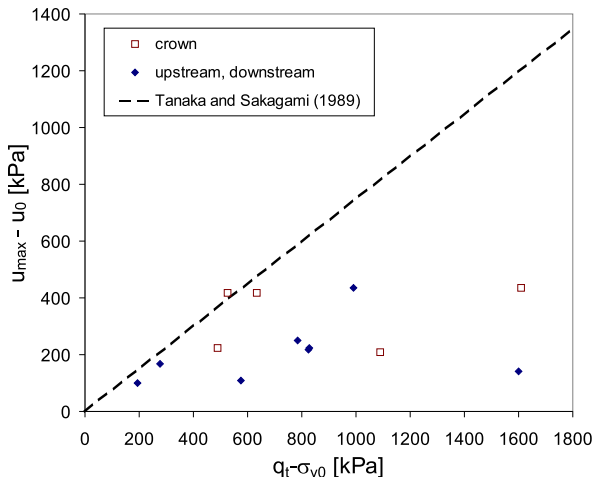


Fig. 4. Verification of Tanaka and Sakagami criterion for soft soil under the embankment

In underconsolidated clays Δu values from CPTU are located above the $0.75(q_t - \sigma_{v0})$ line (Tanaka and Sakagami 1989). Eq. 5 was elaborated for quite homogeneous clay deposits with the thickness exceeding several meters. The presence of sandy or peat inclusions within the mud under the flood embankment can reduce the maximum registered pore pressure – u_{\max} . The maximum pore pressure registered in mud will be smaller than in typical clays.

The majority of the data registered in the soft soil under the flood embankment is located under the criterion proposed by Tanaka and Sakagami (1989). The higher the corrected cone resistance, the greater the distance to the criterion line. The data concerning the dissipation tests in the subsoil confirms that the consolidation is completed in the soft soil under the embankment.

3.2. Stress State and History

Stress state and history in the soft subsoil under the embankment were evaluated with CPTU and DMT data. Soil overconsolidation can be determined from CPTU data according to formula (Lunne et al 1997):

$$OCR = \frac{a(q_t - \sigma_{v0})}{\sigma'_{v0}}, \quad (6)$$

where:

a – coefficient from 0.2 to 0.5 related to plasticity index. According to Mayne et al (1998) this coefficient decreases with plasticity index and void ratio of a given clay. Lunne et al (1997) suggest that the average value of a coefficient is 0.3. Larsson and Mulabdic (1991) propose $a = 0.305$ for intact clays. This correlation can also be refined including the plasticity index of the soil considered. In the present calculation a coefficient equal to 0.3 was assumed,

q_t – corrected cone resistance,

σ_{v0} – total overburden stress.

For the soft soils under the embankment OCR values (Fig. 5) slightly exceeding 1 were found from CPTU. At the embankment toe OCR values from 3 to 4 were obtained. At small depths even higher OCR values are obtained, which could be related either to crust phenomena or to some problems with CPTU test interpretation at small overburden stress, where the probe penetration can not be considered as a loading of deep foundation (Puech and Foray 2002).

Overconsolidation ratio can also be estimated with pore pressure ratio B_q (Lunne et al 1997):

$$B_q = \frac{u_2 - u_0}{q_t - \sigma_{v0}} \quad (7)$$

and some empirical correlations. Parameter B_q calculated with CPTU data under the central part of the embankment (Fig. 6), i.e. for normally consolidated soil, is smaller than typically observed in soft clays (Lunne et al 1997). Less pore pressure is mobilized during cone penetration tests in heterogeneous alluvial soils with the inclusions of a better permeability than in a thick deposit of soft clays.

The analyses are focused on the stress history and state of stress in soft cohesive and organic soils. The following formulae – valid for the soils with material index I_D less than 1.2 – are applied (Marchetti 1980):

– overconsolidation ratio

$$OCR = (0.5K_D)^{1.56}, \quad (8)$$

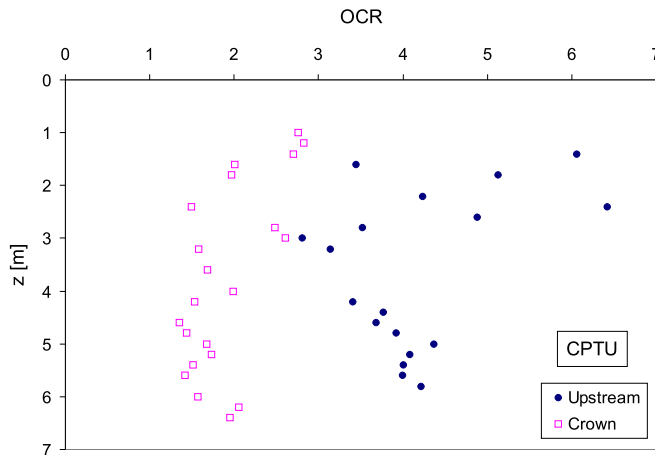


Fig. 5. OCR profiles from the CPTU under the central part and at the embankment toe

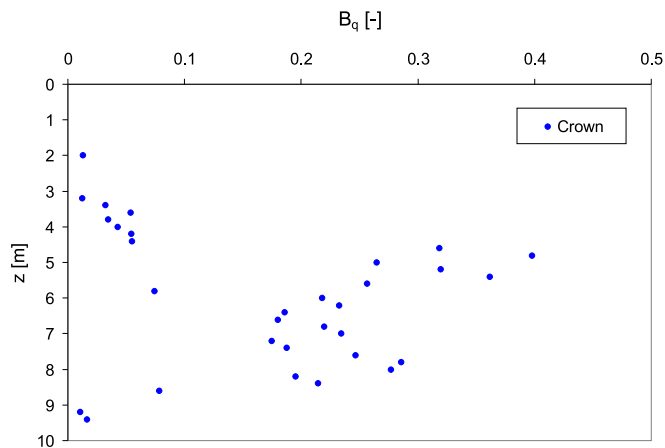


Fig. 6. B_q profile from CPTU soundings under the central part of the embankment



– lateral earth pressure coefficient

$$K_0 = (K_D/1.5)^{0.47} - 0.6. \quad (9)$$

Some other local correlations also exist (Powell and Uglow 1988, Lechowicz, Rabarijoely 1997). The relations for organic soils proposed by Lechowicz, Rabarijoely (1997) are used in this paper:

– overconsolidation ratio

$$OCR = (0.45K_D)^{1.40}, \quad (10)$$

– lateral earth pressure coefficient

$$K_0 = 0.32(K_D)^{0.45}. \quad (11)$$

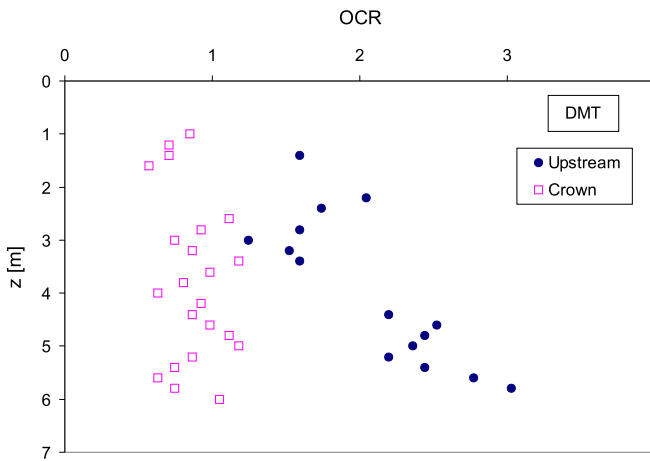


Fig. 7. OCR profiles from the DMT at the crown and at the embankment toe

Values of OCR and K_0 in the soft soil under the central part and at the upstream embankment toe are compared (Fig. 7 and Fig. 8). While overconsolidation ratio close to one is found in the soil under the central part of the embankment, OCR value from 1.5 to 3 is obtained on the upstream side. Earth pressure coefficient K_0 is close to 0.45 in the subsoil under the central part of the embankment and approaches 0.6 for the soft soil at the toe of the embankment (Fig. 8). Profiles of lateral stress index K_D for the soundings at the crown and at the embankment toe are given in Fig. 9. K_D values close to 2 – corresponding to normally consolidated soil – are recorded under the central part of the embankment. At the embankment toe, K_D values are considerably higher than 2 and can

reach 4 or even 5 at greater depths. High K_D at an upstream site are related to crust phenomena and overconsolidation.

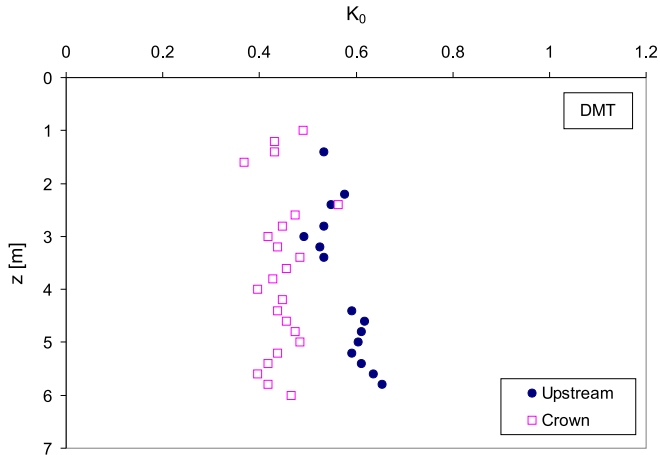


Fig. 8. K_D profiles from the DMT at the crown and at the embankment toe

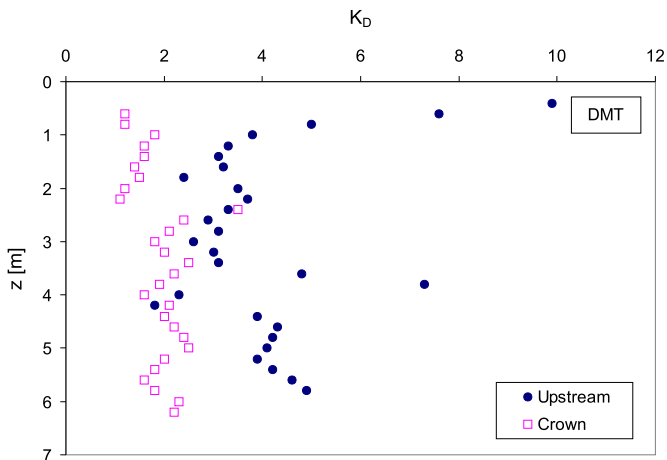


Fig. 9. Lateral stress index K_D for the soundings at the crown and at the embankment toe

Analysis of CPTU and DMT data confirms that the soft soil under the central part of the embankment is normally consolidated, while the soil under the embankment toe is in an overconsolidated state. This overconsolidation is a complex phenomena including mechanical overloading, lateral stress increase due to embankment construction and structural overconsolidation.

4. Dissipation Curve in Normally Consolidated and Overconsolidated Soils

During the cone penetration the nearby soil is subjected to complex loading depending on its position. The measurements of pore water pressure with different filter locations (u_1, u_2, u_3) reflect this complex loading (Sully et al 1999). For the filter located on the tip (u_1 position), the soil is subjected to compressive load and the water pore pressure is mobilized. Generated stress state can be described with spherical cavity expansion. At u_2 position the soil is partially unloaded and is subjected not only to compressive stress but also to shear stress as well. For the filter located behind friction sleeve (u_3 position) the soil is considerably unloaded, the shear deformations within the interface will produce an extra water pressure according to dilatant or contractant soil behaviour. Generated stress state can be modelled here with cylindrical cavity expansion.

In the present tests, a typical CPTU probe with u_2 filter location was used. Pore water pressure u_2 at given depth can be presented (Burns and Mayne 1998):

$$u_2 = u_0 + \Delta u_{oct} + \Delta u_{shear}, \quad (12)$$

where:

- u_0 – equilibrium pore pressure in-situ,
- Δu_{oct} – octahedral component of excess pore pressure corresponding to the zone of plastic soil around the cone tip (see Fig. 10),
- Δu_{shear} – shear-induced component of excess pore pressure generated in the interface.

Octahedric component of excess pore pressure is always positive and decreases during dissipation tests (Mayne 2001). Shear-induced component depends on dilative/contractive behaviour of the soil within interface. It can be negative in overconsolidated or fissured soils or positive in soft normally consolidated soils. Initial pore pressure at the beginning of dissipation can be lower or higher than a hydrostatic one (Fig. 11). When the penetration is stopped a local redistribution of water pore pressure occurs between the zone of predominant compressive stress and the shear stress zone within the interface and the dissipation of the excess water pore pressure begins. As a result of the redistribution, the pore pressure u_2 is initially increasing in overconsolidated soils (dilatory response) and a monotonic decay of pore pressure is observed in normally consolidated soils. According to Kurup and Tumay (1995) an excess pore pressure drop due to normal stress release is observed, when the penetration rate changes abruptly from 2 cm/s to 0 cm/s at the beginning of CPTU dissipation test. This effect should be included in the interpretation of the initial pore pressure at the beginning of dissipation test (see Fig. 13).

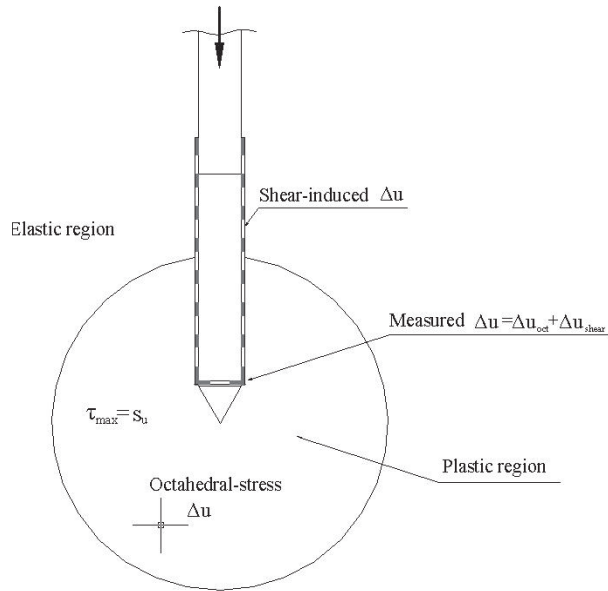


Fig. 10. Soil zones around CPTU probe (Mayne 2001)

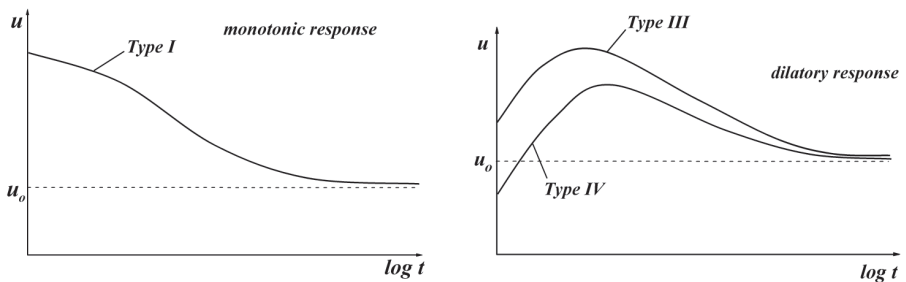


Fig. 11. Typical dissipation curves in normally consolidated and overconsolidated soils (Sully et al 1999)



5. Interpretation of Dissipation Test in Normally Consolidated Soils

Interpretation is based on the cavity expansion theory with critical state soil models, with coupled or uncoupled consolidation analysis. Initial distribution of the pore pressure around the probe is obtained by strain path method (Baligh and Levadoux 1986), large strain finite element analysis (Houlsby and Teh 1988) or cavity expansion (Burns and Mayne 1998, Chang et al 2001). Finite element or finite difference method are used for radial flow and consolidation analysis.

For practical purposes the normalized excess pore pressure is defined (Lunne et al 1997):

$$U = \frac{u_t - u_0}{u_i - u_0}, \quad (13)$$

where:

- u_t – water pore pressure measured in time t ,
- u_0 – equilibrium pore pressure in-situ,
- u_i – initial water pore pressure at the beginning of dissipation $t = 0$.

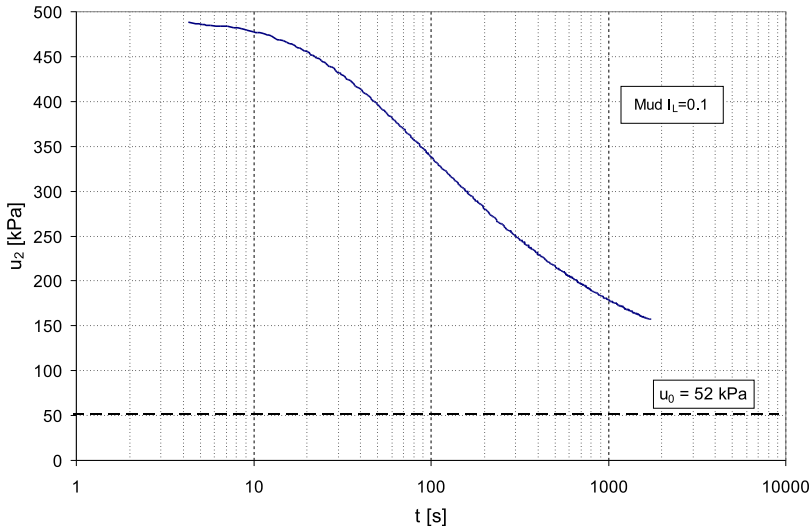


Fig. 12. Typical dissipation curve in NC soils under the embankment

Value of water pressure u_i can be determined by linear extrapolation of the initial portion of dissipation curve plotted in square root time. This procedure should be applied in case of dynamic redistribution of water pressure around the CPTU probe immediately after it stops. An example of the dissipation curve under the central part of the embankment is given in Fig. 12. Extrapolated initial pressure

(see Fig. 13) u_i is equal to 513 kPa. The hydrostatic pore pressure u_0 at the test depth is 52 kPa. The normalized excess water pressure is given in Fig. 14. A set of CPTU dissipation tests performed under the central part of the embankment is given in Fig. 15. Monotonic decrease of excess water pressure observed in dissipation tests under the the central part of the embankment confirms normal consolidation of this subsoil found in CPTU and DMT tests.

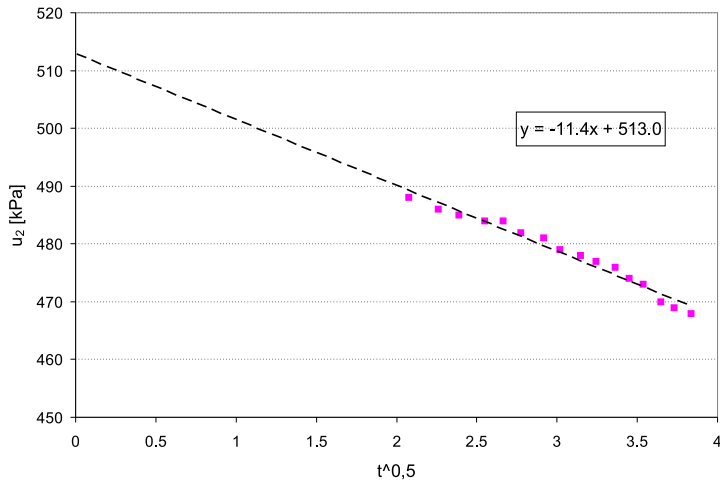


Fig. 13. Determination of the initial pore pressure at the beginning of dissipation test ($t = 0$)

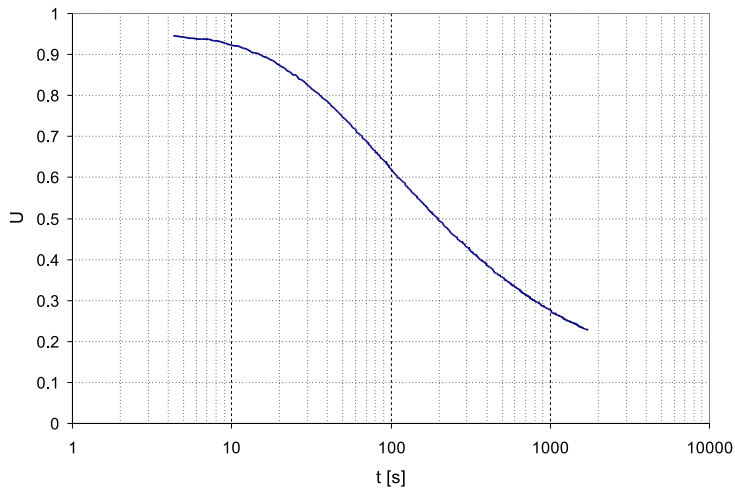


Fig. 14. Normalized excess water pressure



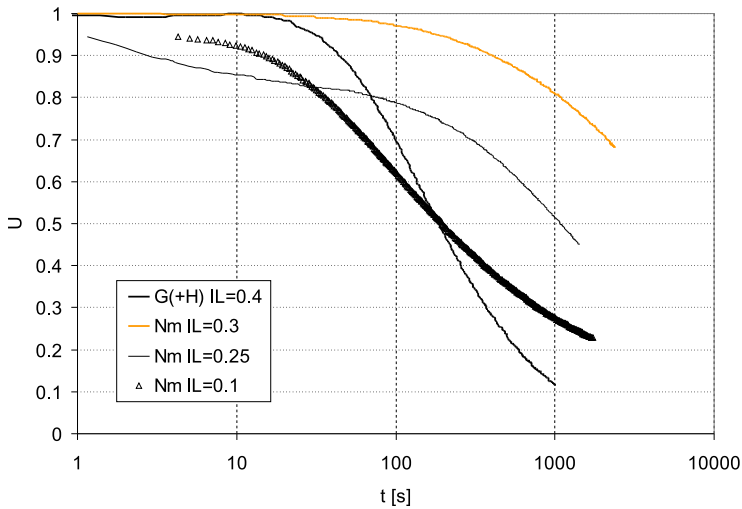


Fig. 15. Set of normalized excess water pressure for the subsoil under embankment

Flow parameters (i.e. coefficient of consolidation and hydraulic conductivity) can be derived from dissipation curves. As the dissipation undergoes predominantly in a horizontal direction, these parameters correspond to the radial flow. The solutions for coefficient of consolidation are generally based on t_{50} – dissipation time for the half of the excess pore pressure. According to Torstensson (Lunne et al 1997):

$$c_h = \frac{T_{50}}{t_{50}} r^2, \quad (14)$$

where:

T_{50} – time factor,

t_{50} – dissipation time for the half of the excess pore pressure,

r – penetrometer radius.

Another solution is proposed for square root time plot of dissipation curve (Teh 1987):

$$c_h = (m/M_1)^2 \sqrt{I_r} r^2, \quad (15)$$

where:

m – initial slope of the linear part for square root time plot of dissipation curve,

M_1 – coefficient equal to 1.15 for the typical (u_2) pore pressure element location,



I_r – rigidity index,

$$I_r = \frac{G}{s_u}, \quad (16)$$

G – shear modulus at the strain level induced in the soil by penetration of the probe,

s_u – undrained shear stress.

Evaluation of rigidity index directly from CPTU tests was proposed (Mayne 2001):

$$I_r = \exp \left[\left(\frac{1.5}{M} + 2.925 \right) \left(\frac{q_t - \sigma_{v0}}{q_t - u_2} \right) - 2.925 \right], \quad (17)$$

where:

q_t – corrected cone resistance,

σ_{v0} – total overburden stress,

M coefficient is determined with triaxial CIU tests (Mayne 2001):

$$M = \frac{6 \sin \phi'}{3 - \sin \phi'}, \quad (18)$$

where:

ϕ' – effective angle of internal friction.

This method demands high quality CPTU tests with high 3rd class of precision. The calculation of M coefficient needs high quality triaxial test on undisturbed samples, which could be problematic and troublesome, especially for organic soils. Alternatively, the rigidity index can be calculated using plasticity index I_p and estimated OCR (Keaveny and Mitchell 1986):

$$I_r \approx \frac{\exp \left(\frac{137 - I_p}{23} \right)}{1 + \ln \left(1 + \frac{(OCR+1)^{3.2}}{26} \right)^{0.8}}. \quad (19)$$

Houlsby and Teh (1988) elaborated another method for evaluation of the consolidation coefficient in a horizontal direction depending on the rigidity index:

$$T' = \frac{c_h t}{r^2 \sqrt{I_r}}. \quad (20)$$



Modified time factor T' depends on porous element location and the normalized excess pore pressure U taken into consideration (Houlsby and Teh 1988). This method gives the most reasonable results, especially when $U = 0.5$ is applied.

In normally consolidated soils the time t_{50} can be used to determine the value of hydraulic conductivity in a horizontal direction (Parez and Fauriel 1988). An empirical correlation is given – Eq. 21 and presented in Fig. 16 together with the soil classification (Parez and Fauriel 1988, Mayne 2001):

$$k_h = (251 \times t_{50})^{-1.25}, \quad (21)$$

where:

t_{50} – is introduced in seconds, and k_h is obtained in cm/s.

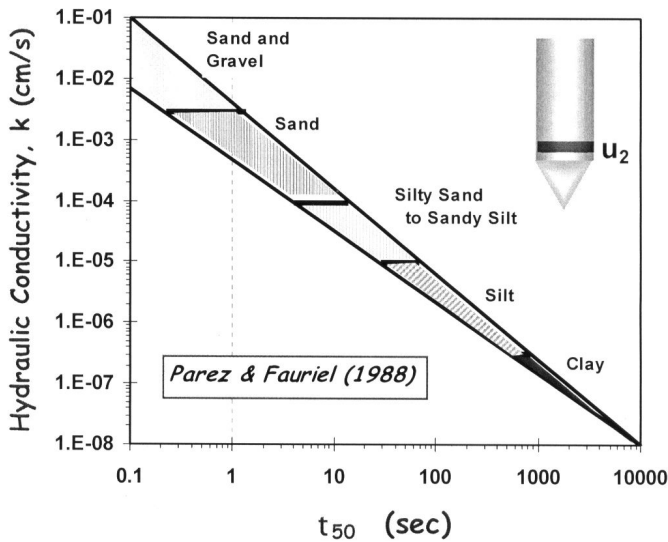


Fig. 16. Parez and Fauriel relation to determine hydraulic conductivity (Mayne 2001)

Robertson et al (1992) proposed a rough estimation of hydraulic conductivity in the horizontal direction as a function of t_{50} . It can also be evaluated from the soil classification chart. The proper evaluation of hydraulic conductivity and consolidation coefficient should also include knowledge of soil anisotropy. Eq. 22 can be used to estimate the consolidation coefficient in a horizontal direction, especially when the in-situ measurements of the constrained modulus from DMT are available:

$$c_h = k_h \frac{M}{\gamma_w}. \quad (22)$$

From the seismic piezocone test the small strain shear modulus (Hegazy and Mayne 1995) and the constrained modulus and hydraulic conductivity (Burns and Mayne 2002) can be derived and consolidation coefficient in horizontal direction can be estimated using Eq. 22. An example of the interpretation of CPTU dissipation test in normally consolidated clays is given by Bałachowski (2006).

6. Interpretation of Dissipation Test in Overconsolidated Soils

A set of dissipation curves registered in the overconsolidated plastic mud at the toe of the embankment is shown on Fig. 17. While in soft plastic mud a monotonic water pressure decay is observed, in plastic mud a dilatory response is found. Direct interpretation of these curves cannot be done, as the classical methods (Lunne et al 1997) concern monotonic dissipation only. The dilatory curves presented in Fig. 17 can be classified as a Type III dissipation curve according to Sully et al (1999) – see Fig. 11.

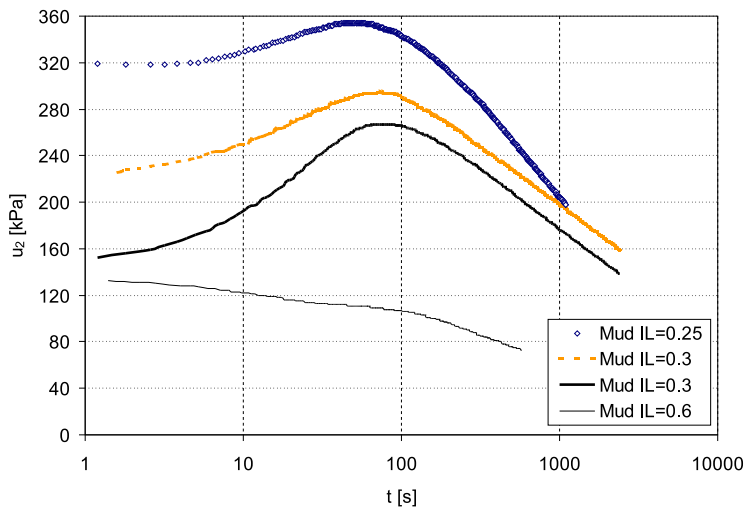


Fig. 17. Set of dissipation curves at the toe of the embankment

There are two different approaches to the interpretation of non-monotonic dissipation curves. The first consists on transferring a dilatory response to the monotonic dissipation case. In the second one the overall dissipation curve with ascending and descending phases is described in one analytical model.

Two correction methods for the transfer of dilatory to monotonic dissipation curve are proposed (Sully et al 1999):

- logarithm of time plot correction (Fig. 18) and
- square root of time plot correction (Fig. 19).

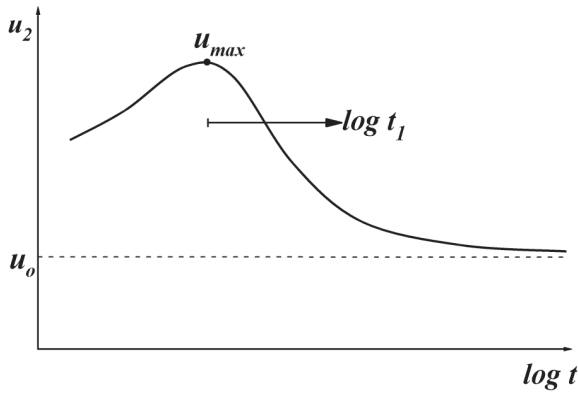


Fig. 18. Logarithm of time plot correction for dilatatory dissipation (Sully et al 1999)

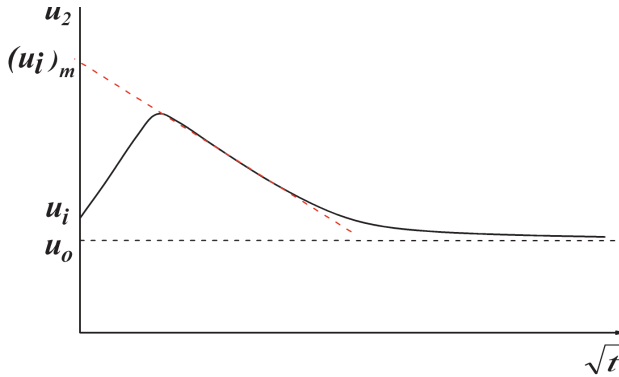


Fig. 19. Square root of time plot correction for dilatatory dissipation (Sully et al 1999)

In the first correction method it is assumed (Fig. 18) that the beginning of the test corresponds to the maximal registered value of water pressure u_{max} , where time is equal zero and the dissipation data are normalized to this maximum. In the square root of time plot correction (Fig. 19), the dissipation after the peak is back-extrapolated to time $t = 0$ in order to obtain the modified maximum initial value of pore pressure $(u_i)_m$. This value is then used to calculate the normalized dissipation curve. The corrected dissipation curves according to the logarithm of time plot correction, are presented in Fig. 20 and the corresponding normalized excess water pressure in Fig. 21. A set of normalized excess water pressure curves with square root of time plot correction is given in Fig. 22.

One should notice that the initial part of the dissipation curve is lost however, when these two correction methods are applied. A new analytical method (Burns and Mayne 1998) describing the overall form of dilatatory response dissipation curve was proposed. Both ascending and descending phases of dissipation curve are

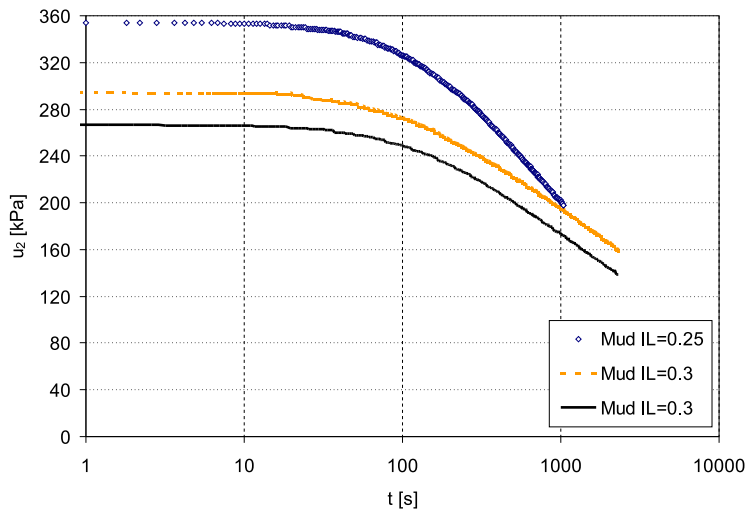


Fig. 20. Dissipation curves with logarithm of time plot correction

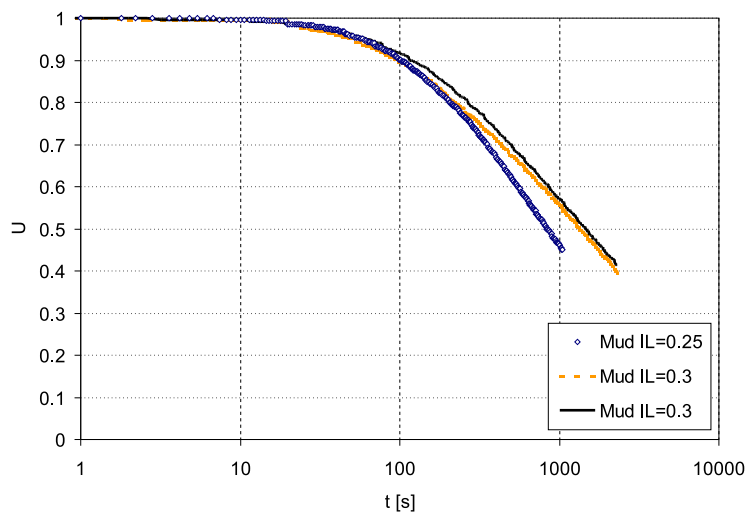


Fig. 21. Normalized excess water pressure curves with logarithm of time plot correction

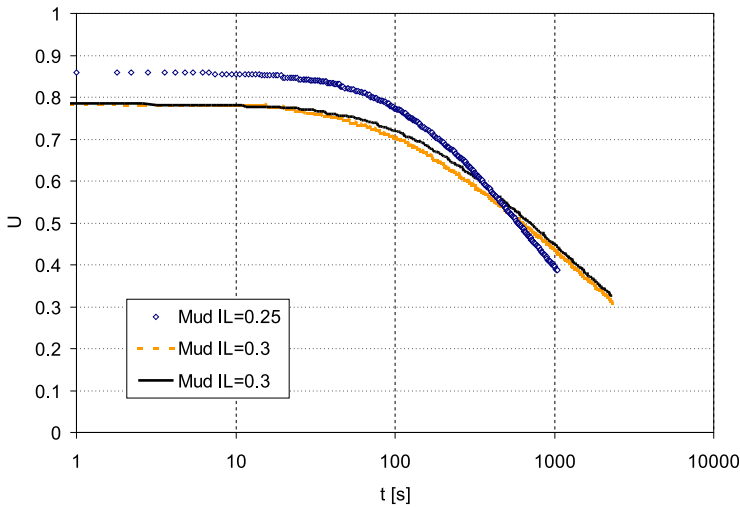


Fig. 22. Normalized excess water pressure curves with square root of time plot correction

analytically obtained with cavity expansion analysis. As an important redistribution of the pore pressure around the probe exists after it is stopped, the initial pore pressure u_i is back-calculated from the initial linear part of the dissipation curve. In normally consolidated soil the model (Fig. 23) gives a monotonic decay of the dissipation curve. In case of dilatatory dissipation the normalized excess water pressure U can exceed 1, especially for highly overconsolidated soils. The modified time factor is proposed as a function of overconsolidation ratio, rigidity index and the angle of internal friction. The calculated normalized excess pore pressure increases with overconsolidation but decreases with angle of internal friction and rigidity index.

The coefficient of consolidation in a horizontal direction is determined from the modified time factor T^* (Mayne 2001):

$$T^* = \frac{c_h t}{r^2 (I_r)^{0.75}}. \quad (23)$$

The pore water dissipation curve at any time t is fitted in Eq. 23 for a given rigidity index. The best fit value of c_h is obtained with trial and error procedure. A closed-form approximate expression for excess water pressure at any time t was proposed (Mayne 2001):

$$\Delta u = \frac{(\Delta u_{oct})_i}{1 + 50T^*} + \frac{(\Delta u_{shear})_i}{1 + 5000T^*}, \quad (24)$$

where:

$(\Delta u_{oct})_i$ – initial octahedral component of excess pore water pressure,



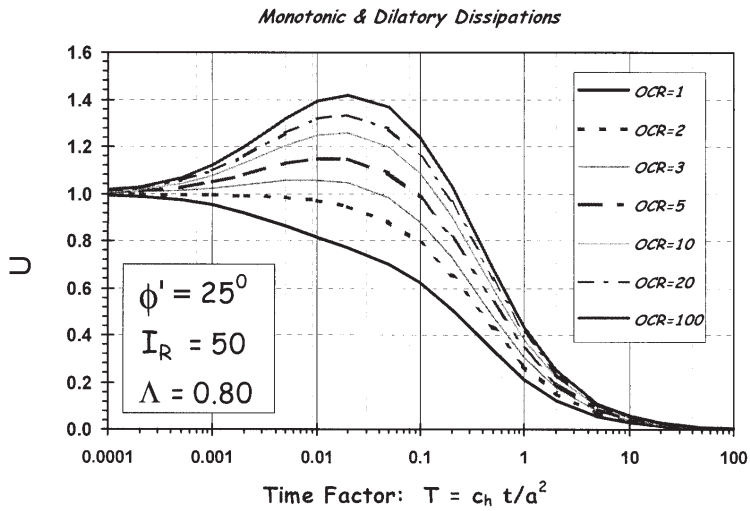


Fig. 23. Normalized excess pore pressure for different *OCR* ratios (Burns and Mayne 1998)

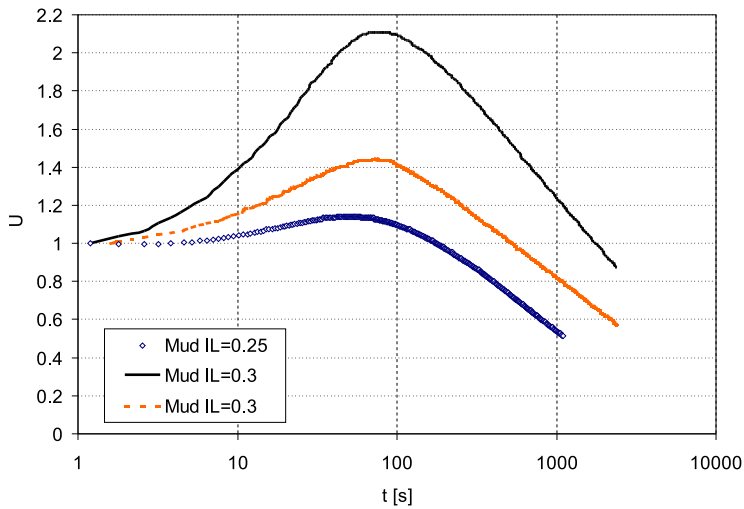


Fig. 24. Set of normalized excess water pressures at the toe of the embankment



$(\Delta u_{shear})_i$ – shear-induced component of the excess pore water pressure at the beginning of dissipation test, determined as follows (Mayne 2001):

$$(\Delta u_{oct})_i = \frac{2}{3} M \sigma'_{v0} (OCR/2)^\Delta \ln I_r, \quad (25)$$

$$(\Delta u_{shear})_i = \sigma'_{v0} [1 - (OCR/2)^\Delta], \quad (26)$$

where:

Δ – plastic volumetric strain ratio.

The evolution of the normalized excess water pressure in plastic mud for soundings at the toe of the embankment is given in Fig. 24. The shape of the curves reflects the stress history and confirms the overconsolidation of the soft subsoil at the toe of the embankment found in CPTU and DMT tests.

7. Conclusions

The stress history in the soft soil under the flood embankment was evaluated from enhanced in-situ tests including CPTU and DMT. While the normally consolidated soil was found under the central part of the embankment the overconsolidated subsoil was detected at the embankment toe. The estimated subsoil overconsolidation is the complex phenomena involving both mechanical overloading and structural effect. Similar *OCR* profiles were obtained using these two penetration tests. DMT test permitted to evaluate the earth pressure coefficient at rest for a given stress history.

The interpretation of CPTU dissipation test is related to stress state and stress history in the soil. Monotonic pore pressure response was found in the dissipation tests performed under the central part of the embankment, where the soil is normally consolidated. Dilatory pore pressure response was observed in overconsolidated subsoil at the embankment toe. The shape of registered dissipation curves is conformed with the stress state and history determined with CPTU and DMT. Dissipation test with a sound knowledge of soil stress history and anisotropy can provide a simple and relatively fast method for in-situ evaluation of the consolidation coefficient and hydraulic conductivity in a horizontal direction. While the interpretation of monotonic dissipation curve is already well established, different interpretation approaches exist for dilatory response. The interpretation of CPTU dissipation test is more difficult in heterogeneous, highly stratified or laminated alluvial soils than in quite uniform clay deposits. Due to soil heterogeneities a larger number of dissipation tests will be necessary to provide a reliable estimation of the hydraulic conductivity and the consolidation coefficient in alluvial soils. The estimation of the flow characteristics in vertical direction will demand some assumptions on the soil anisotropy.



Acknowledgements

The data from CPTU tests performed in the group of professor Zbigniew Sikora was used in this paper. The author would like to thank professor Silvano Marchetti for supplying DMT equipment used in these tests.

References

- Andersen A., Berre T., Kleven A., Lunne T. (1979), Procedures used to obtain soil parameters for foundation engineering in the North Sea, *Marine Geotechnology*, 3(3), 201–266.
- Baligh M. M., Levadoux J. N. (1986), Consolidation after undrained piezocone penetration, Part II: Interpretation, *Journal of Geotechnical Engineering*, ASCE, 112, 727–745.
- Bałachowski L. (2006), Interpretation of CPTU dissipation test in normally consolidated soils, *Inżynieria Morska i Geotechnika*, 1, 32–38 (in Polish).
- Burns S. E., Mayne P. W. (1995), Coefficient of consolidation from type 2 piezocone dissipation in overconsolidated clays, *Proceedings of the Int. Symposium on Cone Penetration Testing*, Vol. 2, Swedish Geotechnical Society, Linköping, Sweden, 137–142.
- Burns S. E., Mayne P. W. (1998), Monotonic and dilatatory pore pressure decay during piezocone tests in clay, *Canadian Geotechnical Journal*, 35, 1063–1073.
- Burns S. E., Mayne P. W. (2002), Interpretation of seismic piezocone results for the estimation of hydraulic conductivity in clays, *Geotechnical Testing Journal*, 25(3), 334–341.
- Chang M. F., Teh C. I., Cao L. F. (2001), Undrained cavity expansion in modified Cam clay II: Application to the interpretation of the piezocone test, *Géotechnique*, 51, No. 4, 335–350.
- Demers D., Leroueil S. (2002), Evaluation of preconsolidation pressure and the overconsolidation ratio from piezocone tests of clay deposits in Quebec, *Canadian Geotechnical Journal*, 39, 174–192.
- Elsworth D. (1993), Analysis of piezocone dissipation data using dislocation methods, *Journal of Geotechnical Engineering ASCE*, 119(10), 1601–1623.
- Hegazy Y. A., Mayne P. W. (1995), Statistical correlations between v_s and CPT data for different soil types, *Proc. Int. Symposium on Cone Penetration Testing*, CPT'95, Linköping, Sweden, 173–178.
- Houlsby G. T., Teh C. I. (1988), Analysis of the piezocone in clay, *Proc. of the International Symposium on Penetration Testing*, ISOPT-1, Orlando, 2, Balkema Pub., Rotterdam, 777–83.
- Kabir M. G., Lutenegeger A. J. (1990), In situ estimation of the coefficient of consolidation of clays, *Canadian Geotechnical Journal*, 27, 58–67.
- Keaveny J. M., Mitchell J. K. (1986), Strength of fine-grained soils using the piezocone, *Proc. of ASCE Special Conference In Situ 86*, Blacksburg, 668–685.
- Kulhawy F. H., Mayne P. W., Kay J. N. (1990), Observations on the development of pore water stresses during piezocone penetration in clays, *Canadian Geotechnical Journal*, 27, 418–428.
- Kurup P. U., Tumay M. T. (1995), Piezocone dissipation curves with initial excess pore pressure variation, *Proc. Int. Symposium on Cone Penetration Testing*, CPT'95, Linköping, Sweden, 195–200.
- Larsson R., Mulabdic M. (1991), *Piezocone Tests in Clay*, Swedish Geotechnical Institute, Linköping, Report, 42.
- Lechowicz Z., Rabarijoely S. (1997), *Organic Subsoil Evaluation on DMT Tests*, Archives of Wydział Melioracji i Inżynierii Środowiska, SGGW (in Polish).
- Lechowicz Z., Szymański A. (2002), *Deformation and Stability of the Embankments on Organic Soils*, Part I, SGGW Publication, Warsaw (in Polish).



- Lunne T., Robertson P. K., Powel J. J. M. (1997), *Cone Penetration Testing in Geotechnical Practice*, Blackie Academic and Professional.
- Marchetti S. (1980), In situ tests by flat dilatometer, *Journal of the Geotechnical Engineering Division*, ASCE, Vol. 106, No. GT3, 299–321.
- Marchetti S., Monaco P., Totani G., Calabrese M. (2001), The flat dilatometer test (DMT) in soil investigations. A report by the ISSMGE Committee TC16, *Proc. IN SITU 2001*, Bali, May 21, 41 p.
- Marchetti S., Monaco P., Totani G. (2004), Discussion of “Consolidation and permeability properties of Singapore marine clay” by J. Chu, Myint Win Bo, M. F. Chang and V. Choa, *Journal of Geotechnical and Geoenvironmental Engineering*, ASCE, 130, No. 3, 339–340.
- Mayne P. W., Robertson P. K., Lunne T. (1998), Clay stress history evaluated from seismic piezocone tests, *Proc. Geotechnical Site Characterization*, Robertson and Mayne (eds), Balkema, Rotterdam, 1113–1118.
- Mayne P. W., Burns S. E. (2000), An approach to evaluation of field CPTU dissipation data in overconsolidated fine-grained soils, Discussion, *Canadian Geotechnical Journal*, 37, 1395–1397.
- Mayne P. W. (2001), Stress-strain-strength-flow parameters from enhanced in-situ tests, *Proc. IN SITU*, Bali, May 21, 27–48.
- Młynarek Z. (2003), Current trends for in-situ determination of soil parameters – part I, *Inżynieria Morska i Geotechnika*, No. 6, 377–383 (in Polish).
- Młynarek Z. (2004), Current trends for in-situ determination of soil parameters – part II, *Inżynieria Morska i Geotechnika*, No. 1, 22–28 (in Polish).
- Parez L., Fauriel R. (1988), Advantages from piezocone application to in-situ tests, *Révue Française de Géotechnique*, 44, 13–27 (in French).
- Powell J. J. M., Uglow I. M. (1988), Marchetti dilatometer testing in UK soils, *Proc. Int. Sym. on Penetration Testing*, Orlando, 1, 555–562.
- Puech A., Foray P. (2002), Refined model for interpreting shallow penetration CPTs in sands, *Proc. Offshore Technology Conference*, Houston, Texas U.S.A., 6–9 May, Paper No. 14275.
- Robertson P. K., Sully J. P., Woeller D. J., Lunne T., Powell J. J. M., Gillespie D. G. (1992), Estimating coefficient of consolidation from piezocone tests, *Canadian Geotechnical Journal*, 29, 539–550.
- Sikora Z., Michalak R., Bałachowski L. (2004), CPTU sounding of the subsoil under the road embankment, *Proc. Conference Współpraca budowli z podłożem gruntowym*, t. 1, Białowieża 17–18 czerwca, 215–223 (in Polish).
- Sully P. J., Robertson P. K., Campanella R. G., Woeller D. J. (1999), An approach to evaluation of field CPTU dissipation data in overconsolidated fine-grained soils, *Canadian Geotechnical Journal*, 36, 369–381.
- Tanaka Y., Sakagami T. (1989), Piezocone testing in underconsolidated clay, *Canadian Geotechnical Journal*, 26, 563–567.
- Teh C. I. (1987), *An Analytical Study of the Cone Penetration Test*, D. Phil. thesis, Oxford University.
- Teh C. I., Housley G. T. (1991), An analytical study of the cone penetration test in clay, *Géotechnique*, 41, 17–34.
- Wolski W. (1988), Geotechnical properties of peats and peaty soils. Methods of their determination, General report, *Proc. 2nd Baltic Conf. On Soil Mechanics and Foundation Eng.*, Tallin.

